

Influence of spin-orbit interaction within the insulating barrier on the electron transport in magnetic tunnel junctions

A. Vedyayev,^{1,2,*} N. Ryzhanova,^{1,2} N. Strelkov,^{1,2} M. Titova,¹ M. Chshiev,² B. Rodmacq,² S. Auffret,² L. Cuchet,² L. Nistor,³ and B. Dieny^{2,†}

¹*Department of Physics, Moscow Lomonosov State University, Moscow 119991, Russia*

²*SPINTEC, Université Grenoble Alpes, CEA, Centre National de la Recherche Scientifique, 38000 Grenoble, France*

³*Applied Materials, 38000 Grenoble, France*

(Received 26 August 2016; revised manuscript received 25 January 2017; published 21 February 2017)

We present a theory of the anisotropy of tunneling magnetoresistance (ATMR) phenomenon in magnetic tunnel junctions (MTJs) attributed to Rashba spin-orbit interaction in the insulating barrier. ATMR represents the difference of tunnel magnetoresistance (TMR) amplitude measured with in-plane and out-of-plane magnetic configurations. It is demonstrated that within the spin-polarized free-electron model the change of conductance associated with the ATMR is exactly twice the change of conductance measured at full saturation (i.e., in parallel configuration of magnetizations) between in-plane and out-of-plane configuration, i.e., the tunneling anisotropic magnetoresistance (TAMR). Both ATMR and TAMR are closely related to the TMR amplitude and spin-orbit constant. The predicted ATMR phenomenon is confirmed experimentally, showing a few percent value in the case of the widely studied CoFeB/MgO/CoFeB based MTJ.

DOI: [10.1103/PhysRevB.95.064420](https://doi.org/10.1103/PhysRevB.95.064420)

Spin-orbit interactions (SOIs) are at the origin of several transport properties of bulk ferromagnetic metals, such as anomalous Hall effect (AHE) [1,2] and anisotropic magnetoresistance [3]. More recently a lot of attention has been paid to the influence of spin-orbit coupling (Rashba [4] or spin Hall effect [5]) on the nonequilibrium spin-orbit torque in single nanomagnets [4] and on the tunneling anisotropic magnetoresistance (TAMR) of magnetic tunnel junctions (MTJs) [6–9]. The TAMR phenomenon in MTJs is usually measured at full saturation of the MTJ and consists in a variation of the tunnel resistance in parallel magnetic configuration as a function of the direction of the magnetization with respect to the crystallographic axis. It is measured either under a rotating saturation field in tunnel junctions with two magnetic electrodes [9] or in junctions with only one ferromagnetic [10–12] or antiferromagnetic [13] electrode. The TAMR is of a different origin compared to TMR [14]. One origin of TAMR [6,7,10,15] is the Rashba interaction which arises from the gradient of electrical potential at the interfaces between the ferromagnetic layer and nonmagnetic heavy metal, semiconductor, or insulator layer. It was shown that this type of SOI influences the interfacial density of states (DOS) in the ferromagnetic layer resulting in a dependence of the DOS on the direction of the magnetization vector with respect to the crystallographic axes. As a result, the tunneling current depends on the angle between the magnetization and crystallographic axes.

In this paper, we present a theoretical and experimental study of the anisotropy of the TMR (ATMR) in magnetic tunnel junctions in the presence of Rashba SOI within the tunnel barrier. The ATMR in MTJs differs from the TAMR as follows. Let us define R_{xP} , R_{xAP} (R_{zP} , R_{zAP}) as the MTJ resistances in parallel (P) and antiparallel (AP)

configuration with the magnetization of the two electrodes being in plane (x direction) [out of plane (z direction)]. The TAMR is defined as $TAMR = TAMR_P = (R_{zP} - R_{xP})/R_{xP}$. It is usually measured in parallel magnetic configuration. It can also be defined as $TAMR_{AP}$ in antiparallel configuration, i.e., $TAMR_{AP} = (R_{zAP} - R_{xAP})/R_{xAP}$. In contrast, in this paper, we introduce the ATMR defined as

$$ATMR = \frac{R_{xAP} - R_{xP}}{R_{xP}} - \frac{R_{zAP} - R_{zP}}{R_{zP}}. \quad (1)$$

Considering that the $TAMR_P$ is weak [9], $ATMR \sim TAMR_P - TAMR_{AP}$. The ATMR represents the variation of the TMR amplitude between in-plane magnetic configuration and out-of-plane magnetic configuration due to SOI. It is interesting to note that such dependence of the magnetoresistance amplitude on the direction of the current with respect to the magnetization has already been observed with the giant magnetoresistance in spin valves [16]. In MTJs, from a general experimental point of view, the TMR of MgO based in-plane magnetized MTJs has reached values above 600% [17,18]. In contrast, the largest TMR of MgO based out-of-plane magnetized MTJs is in the range 200–350% [19], significantly lower than the values obtained in their in-plane magnetized counterparts. In theory, the TMR amplitude predicted by *ab initio* calculations neglecting spin orbit [14] is much larger than the experimentally obtained values. In experiments, the TMR amplitude is limited by defects which can have several origins: interdiffusion of metallic species in the composite magnetic electrodes [17,18,20], structural defects associated with fcc/bcc in-stack structural competition [21], presence of dislocations in MgO associated with Fe(Co)-MgO crystallographic mismatch, adsorbed water molecules, etc.

However, considering the significant difference of TMR observed between in-plane and out-of-plane magnetized MTJs, it is interesting to investigate whether an intrinsic origin of this difference can be attributed to spin-orbit effects. In this paper, we developed an analytic description of ATMR in the free-electron model as it was carried out in Ref. [22] for TMR

*vedy@magn.ru

†bernard.dieny@cea.fr

and show that correlations exist between ATMR, TAMR, and TMR. Furthermore, we confirm our theoretical predictions by experimental investigation of the ATMR behavior in MgO based MTJs with orthogonal anisotropies, i.e., with one electrode being magnetized in plane and the other being magnetized out of plane. By applying a saturation field successively in plane then out of plane, we could derive the ATMR amplitude in these MgO based MTJs. Its amplitude is quite weak, which is consistent with earlier TAMR measurements on similar MTJs [9], and the TAMR_{AP} is found to be opposite to the TAMR_P.

In MTJs, spin-orbit coupling appears within the barrier due to the gradient of voltage across the barrier (Rashba effect) or due to the presence of impurities of heavy ions embedded into the barrier. In the MgO based MTJs of practical interest, in particular for magnetic random access memories, the amount of heavy metal impurities in the tunnel barrier is negligible so that the dominant source of spin-orbit coupling is in this case the Rashba effect.

Earlier, the AHE in MTJs due to the spin-orbit scattering in the barrier [23] or Rashba type spin-orbit coupling [24] were investigated. Here below, the influence of spin-orbit coupling due to the gradient of voltage within the barrier (Rashba effect) on the tunnel magnetoresistance of MTJs and on the anisotropy of this TMR is theoretically addressed. Let us describe the MTJ as a magnetic sandwich consisting of two ferromagnetic metals separated by an insulating barrier. The Hamiltonian of the system can be written for the free-electron model in mean-field approximation as follows:

$$\hat{H} = \frac{\hat{p}^2}{2m} - J_{sd} \hat{\sigma} \langle \hat{S}_d \rangle \quad (2)$$

for the F layer, where J_{sd} is the exchange interaction of the itinerant s electrons with the localized d electrons, $\hat{\sigma}$ is the Pauli matrix, and $\langle \hat{S}_d \rangle$ is the averaged value of d -electron spin described as a unit vector in the direction of the local magnetization:

$$\langle \hat{S}_d \rangle = (\sin \theta \cos \varphi; \sin \theta \sin \varphi; \cos \theta). \quad (3)$$

In the barrier, the Hamiltonian is written

$$\langle \hat{H} \rangle = \frac{\hat{p}^2}{2m} + U + i\alpha \left(\vec{\sigma} \left[\vec{z} \times \frac{\partial}{\partial \vec{r}} \right] \right), \quad (4)$$

where $\alpha = \lambda^2 eV/d$, λ being the effective Compton length, d is the barrier thickness, U is its height, V is the drop of applied voltage across the barrier, and \vec{z} is the unit vector in the z direction (see Fig. 1). The solutions of the Schrödinger equation with Hamiltonians (2)–(4) for the wave functions in all three layers for $\theta = \pi/2$ or 0 and $\varphi = 0$ can be easily derived.

We now calculate the densities of currents J at first order on voltage for both directions of spin projections substituting the calculated expressions for the wave functions into the expression

$$J^{\uparrow(\downarrow)} = -\frac{e^2}{2\pi\hbar} \frac{1}{(2\pi)^2} \int J_{\kappa,\varepsilon,\gamma}^{\uparrow(\downarrow)} \frac{\partial f}{\partial \varepsilon} d\gamma d\varepsilon \kappa d\kappa, \quad (5)$$

$$J_{\kappa,\varepsilon,\gamma}^{\uparrow(\downarrow)} = \text{Im} \psi^* \frac{\partial \psi}{\partial z},$$

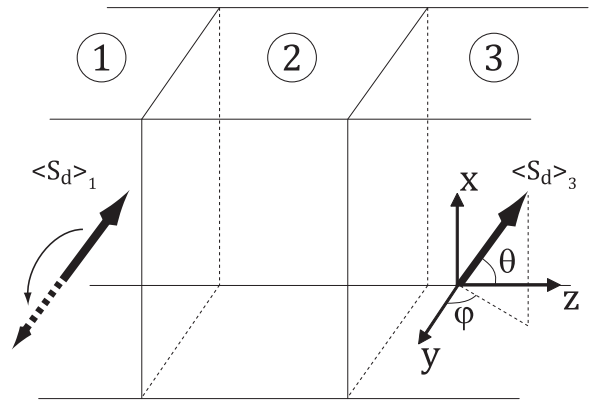


FIG. 1. Sandwich structure. 1 and 3, ferromagnetic layers; 2, insulator. Averaged spin $\langle \hat{S}_d \rangle_1$ is collinear (P or AP) to the $\langle \hat{S}_d \rangle_3$.

where $J_{\kappa,\varepsilon,\gamma}^{\uparrow(\downarrow)}$ is the dimensionless partial current density for spin-up and -down projections and for given values κ , ε and angle γ .

We are interested in the value of the tunneling anisotropic magnetoresistance (TAMR) and anisotropy of tunnel magnetoresistance (ATMR). In the limit of a thick barrier, we have

$$\begin{aligned} \Delta J_{\text{TAMR}}^{\text{P(AP)}} &= J_{\kappa,\varepsilon} |_{\theta=\frac{\pi}{2}, \varphi=0} - J_{\kappa,\varepsilon} |_{\theta=0, \varphi=0} \\ &= \pm (\Delta E)^2 \frac{8q_0^2 e^{-2q_0 d} (q_0^2 - k_1 k_2)^2}{(q_0^2 + k_1^2)^2 (q_0^2 + k_2^2)^2} (k_1 - k_2)^2 \\ &= \pm (\Delta E)^2 \frac{1}{2} \text{TMR}, \\ \Delta E &= E_+|_{z=z_2} - E_-|_{z=z_2} \approx \frac{2m}{\hbar^2} \frac{d}{q_0} \alpha |\kappa| \end{aligned} \quad (6)$$

where TMR is the amplitude of the tunnel magnetoresistance expressed as $(J^{\text{P}} - J^{\text{AP}})$ for a given voltage, without spin-orbit contributions:

$$\begin{aligned} E_{\pm}(z) &= e^{q_{\pm}(z-z_1)}, \\ q_{\pm} &= \sqrt{q_0^2 \pm \frac{2m}{\hbar^2} \alpha |\kappa|}, \\ q_0^2 &= \frac{2m}{\hbar^2} (U - E_F + \varepsilon) + \kappa^2, \\ k_{1(2)} &= \sqrt{k_F^{\uparrow(\downarrow)2} - \kappa^2 - \frac{2m}{\hbar^2} \varepsilon}, \end{aligned}$$

where E_F is the Fermi energy. The difference of $q_+ - q_-$ is due to the splitting of the evanescent bands in the barrier caused by SOI. In Eq. (6), it is interesting to note that $\Delta J_{\text{TAMR}}^{\text{P}}$ is exactly opposite to $\Delta J_{\text{TAMR}}^{\text{AP}}$. As a result, the following remarkable equality is obtained

$$\begin{aligned} \Delta J_{\text{ATMR}} &= (J^{\text{P}} - J^{\text{AP}})|_{\theta=\frac{\pi}{2}, \varphi=0} \\ &\quad - (J^{\text{P}} - J^{\text{AP}})|_{\theta=0, \varphi=0} = 2\Delta J_{\text{TAMR}}^{\text{P}} \end{aligned} \quad (7)$$

meaning that the ATMR amplitude is twice the TAMR amplitude. Besides equation (6) indicates that the TAMR is proportional to TMR before integration over ε and κ , so that the TAMR/TMR ratio gives the value of the spin-orbit amplitude α . For a given α , the larger the TMR, the larger

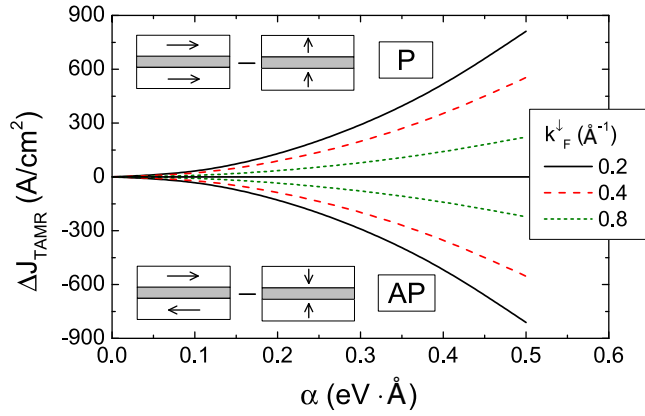


FIG. 2. The dependence of the absolute TAMR ($J_{\theta=\pi/2} - J_{\theta=0}$) at a given voltage $V = 0.5$ V on the value of Rashba constant α . For $\theta = \pi/2$, the direction of magnetization is perpendicular to the current (in-plane magnetization) and for $\theta = 0$ it is parallel to the current (out-of-plane magnetization). The upper half of the figure corresponds to the configuration with parallel directions of magnetizations of F electrodes (magnetic configurations shown in top inset) and the lower half corresponds to the antiparallel one (magnetic configurations shown in bottom inset). The curves are given for different values of k_F^\perp (\AA^{-1}) and fixed $k_F^\parallel = 1 \text{ \AA}^{-1}$, $q_0 = 1 \text{ \AA}^{-1}$, $d = 7 \text{ \AA}$. The values of constant α are given in Table I of [4]. They vary in the interval 0.01–1.

the TAMR. The most dramatic changes in electron transport due to the influence of spin-orbit interaction are expected in MTJs comprising half-metallic ferromagnetic electrodes. In this case, in the antiparallel magnetic configuration, the density of current without spin-orbit interaction is equal to zero. In the presence of SOI, a tunneling current appears the density of which is proportional to the square of the spin-orbit interaction $(\Delta E)^2$. As a result, the tunnel magnetoresistance $(J^P - J^{AP})/J^{AP}$ remains finite. For weak values of α in the range 0.01–0.1 eV Å, the TMR should reach very large amplitude in the range 10^3 – 10^5 . However, in experiments, TMR amplitude of only $\sim 850\%$ at low T was observed [25]. This rather low experimental TMR value obtained in half-metal based MTJs can be explained by the presence of significant SOI. Another interesting feature of the influence of spin-orbit interaction on TAMR for the antiparallel configuration of half-metallic electrodes is the expected abnormally high value of anisotropic magnetoresistance in AP configuration: $J^{AP}(\theta = 0)/J^{AP}(\theta = \pi/2) = 2$. Figure 2 shows the variation of the absolute TAMR in the P and AP configurations versus Rashba constant α for different values of k_F^\perp for fixed k_F^\parallel . As already pointed out, the signs of TAMR are opposite for the P and AP configurations. We may notice that the absolute values of TAMR (ΔJ_{TAMR}) for P and AP configurations are the same, but the absolute relative value of TAMR defined as $\Delta J_{\text{TAMR}}/J_{\theta=0}$ is larger in the AP configuration due to the difference of total currents for P and AP configurations.

The TAMR in MgO- and Al_2O_3 -based MTJs has already been measured in Ref. [9] in parallel magnetic configuration by applying a rotating field large enough (7 T) to saturate the magnetization of both electrodes along the field direction.

A well-defined TAMR signal was observed at 10 K with, however, a rather small amplitude in the range 0.1–0.3%. In the present experimental study, the ATMR of MgO-based MTJs was investigated. Measuring the ATMR requires us to be able to set the sample in AP and P magnetic configurations, the magnetization of both magnetic electrodes being once oriented in plane and once oriented out of plane. Practically, this is possible in P configuration by applying a saturation field, respectively, in plane and out of plane. However, achieving this for the AP configuration would require the sample to exhibit a strong cubic anisotropy with easy axis both out of plane and in plane or an antiferromagnetic coupling through the tunnel barrier larger than the anisotropy energy. None of these requirements are satisfied in sputtered CoFeB/MgO-based MTJs. We therefore decided to design a sample in which the two magnetic electrodes have orthogonal anisotropies: one has out-of-plane anisotropy, and the other has easy-plane anisotropy. This can be obtained by carefully adjusting the thickness of each CoFeB layer so that in one electrode the interfacial perpendicular magnetic anisotropy (PMA) at the CoFeB/MgO interface dominates the demagnetizing energy of the corresponding CoFeB layer, whereas for the other electrode the opposite is true. Then by performing two sets of magnetoresistance measurements versus field, using the current-in-plane tunneling setup (CIPTMR) [26], one with field applied in plane and the other with field out of plane up to full saturation, one can probe on the same sample the TMR amplitude associated with a change in relative orientation of magnetization from 90 to 0° with the parallel final state either in plane or out of plane. Here one must make sure that the full saturation can be reached with the maximum fields available in the CIPTMR measurement setup both with in-plane and out-of-plane field. In our setups, these maximum fields are, respectively, $H_{x \text{ max CIPTMR}} = 1.5$ kOe for the in-plane field configuration and $H_{z \text{ max CIPTMR}} = 3$ kOe for the out-of-plane field configuration. As a result, the thicknesses of the two magnetic electrodes (t_1 and t_2) must be chosen to fulfill the following equations:

$$0 < \frac{2}{M_{1s}} \left(\frac{K_{1s}}{t_1} - 2\pi M_{1s}^2 \right) < H_{x \text{ max CIPTMR}},$$

$$0 < \frac{2}{M_{2s}} \left(2\pi M_{2s}^2 - \frac{K_{2s}}{t_2} \right) < H_{z \text{ max CIPTMR}}, \quad (8)$$

where M_s , K_s , and t represent, respectively, the saturation magnetization, interfacial PMA, and thickness of the two magnetic electrodes. After a detailed study of the influence of the electrode thickness on the magnetic effective anisotropy of bottom and top electrodes [27], the following sample composition was chosen fulfilling the required conditions: Ta (3 nm)/CoFeB (1.15 nm)/MgO (1.4 nm)/FeCoB (1.6 nm)/Ta (1 nm)/Pt (2 nm). The MgO barrier was formed by a two step natural oxidation of an Mg layer under 150 mbars oxygen for 10 s. The samples were subsequently annealed 1 h at 300 °C. The 1.15-nm-thick bottom electrode which has a weaker interfacial anisotropy (Co rich alloy) has in-plane magnetization (electrode 2) whereas the thicker top electrode which is Fe rich has out-of-plane anisotropy (electrode 1).

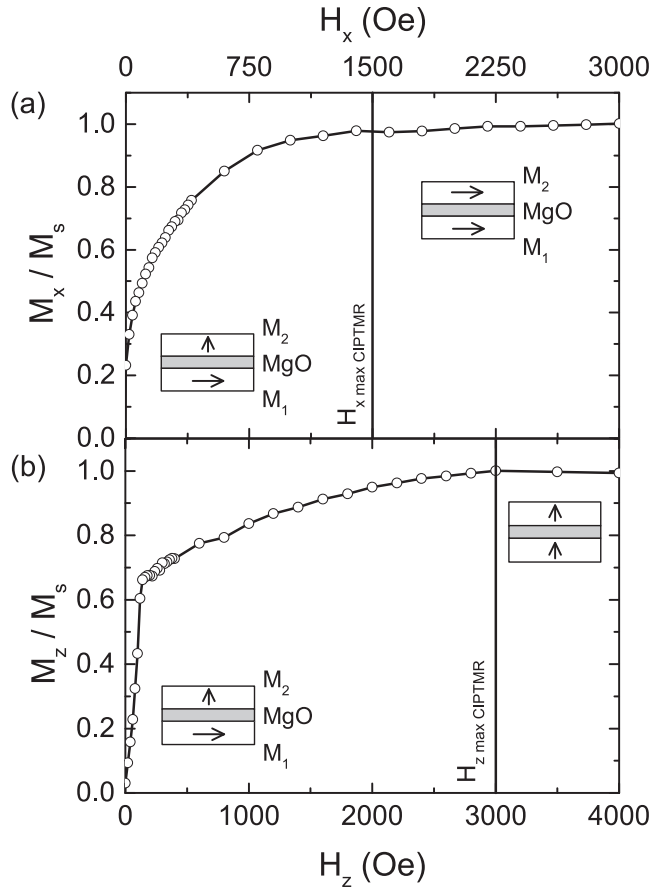


FIG. 3. Normalized magnetization vs field. (a) Field applied in plane (x direction). (b) Field applied out of plane (z direction). The vertical lines indicate the corresponding maximum field available in the CIPTMR experimental setups.

Magnetization measurements were first performed using a vibrating sample magnetometer with in-plane and out-of-plane field (see Fig. 3). Figure 3(a) shows that in-plane saturation of the top electrode magnetization is reached at about 1.3 kOe, below the 1.5-kOe maximum field available in the CIPTMR setup with in-plane field configuration. Conversely, Fig. 3(b) indicates that the out-of-plane saturation of the bottom electrode is reached at a field ~ 3 kOe low enough so that saturation can be reached in the CIPTMR setup with out-of-plane field configuration. The rapid rise of magnetization at low fields (< 0.1 kOe) seen in Fig. 3(b) is due to the fact that the top electrode at $H_z = 0$ is in multidomain up and down states and rapidly gets saturated out of plane upon H_z field application.

Next, CIPTMR measurements were performed with field applied in plane and out of plane up to full saturation (see Fig. 4). A gradual decrease of the resistance is observed in both cases due to the change in relative orientation between the magnetization of the two electrodes from 90° to 0° . By combining the data of Figs. 3 and 4, we plotted in the insets the variation of conductance (inverse of resistance) versus the component of rotating magnetization along the applied field direction.

Assuming that the conductance varies as a linear function of the scalar product between the magnetization of the two

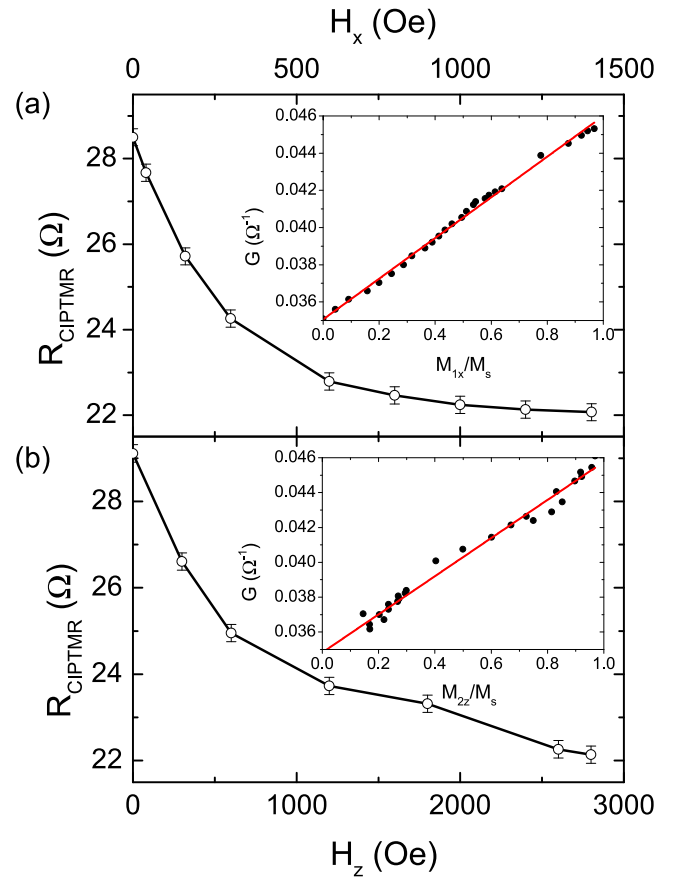


FIG. 4. R_{CIPTMR} vs field. (a) Field applied in plane (x direction). (b) Field applied out of plane (z direction). Inset: Conductance (inverse of R_{CIPTMR}) vs the reduced component of the rotating magnetization along the applied field direction. The red line represents a linear fit of the experimental variation.

electrodes [22], linear fittings of the conductance versus component of the rotating magnetization along field direction were performed forcing the conductance at $H = 0$ to be the same in the two cases. The following fitting equations were obtained: $G(\Omega^{-1}) = (0.034984 \pm 8 \times 10^{-5}) + (0.01106 \pm 7 \times 10^{-4})M_{1x}/M_s$ for in-plane field [Fig. 4(a)] and $G(\Omega^{-1}) = (0.034984 \pm 8 \times 10^{-5}) + (0.01071 \pm 1.4 \times 10^{-4})M_{2z}/M_s$ for out-of-plane field. From these values, by extrapolation, one can derive the full TMR amplitude measured between P and AP configurations in in-plane and out-of-plane configurations. The following values were obtained: $R_{x \text{ min}} = 21.72 \pm 0.15 \Omega$ and $R_{x \text{ max}} = 41.80 \pm 0.29 \Omega$ yielding $(\Delta R/R)_x = 92.4 \pm 0.8\%$ for the in-plane configuration and $R_{z \text{ min}} = 21.88 \pm 0.29 \Omega$ and $R_{z \text{ max}} = 41.20 \pm 0.55 \Omega$ for the out-of-plane configuration yielding $(\Delta R/R)_z = 88.3 \pm 23\%$.

It appears clearly from these results that the difference of TMR measured in plane and out of plane is weak. Therefore the large difference in TMR amplitude generally observed between in-plane magnetized MTJs (up to 600% at RT) and out-of-plane magnetized MTJs (up to 350%) is due not to an intrinsic effect related to spin-orbit coupling but likely to a poorer growth quality in out-of-plane magnetized MTJs due to the in-stack coexistence of fcc and bcc layers or to the use

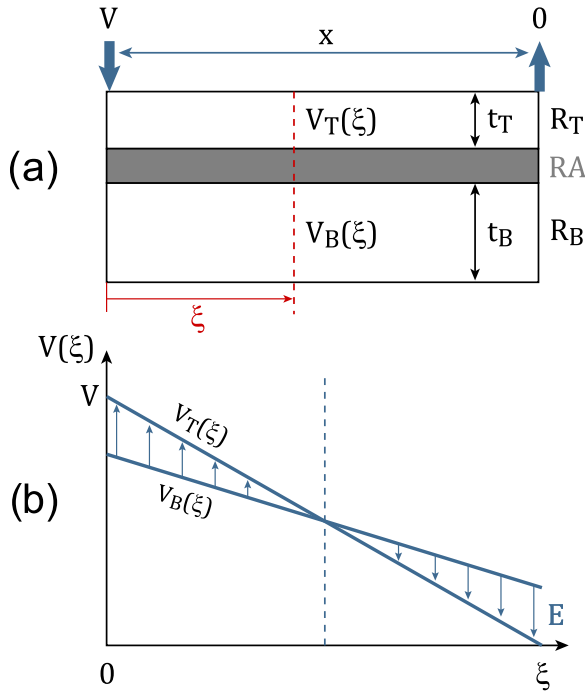


FIG. 5. (a) Toy model as in Fig. 1 of Ref. [26] for the CIPTMR experiment. (b) Spatial variation of the voltage in the top electrode $V_T(\xi)$ and in the bottom electrode $V_B(\xi)$, ξ being the in-plane coordinate between the two electrical contacts. The voltage drop across the barrier to which the Rashba coefficient is proportional is represented by the vertical separation $V_T(\xi) - V_B(\xi)$.

of thinner magnetic layers in perpendicular MTJs or to the presence of impurities in or very next to the tunnel barrier.

More quantitatively, the error bars are unfortunately too large to make a definite conclusion but the observed difference between $R_{z\min}$ and $R_{x\min}$ is consistent in amplitude (a few tenths of a percent) and sign with the previous measurement of TAMR reported in Ref. [9]. Furthermore the TAMRs measured in P and AP configurations ($R_{z\min} - R_{x\min}$ versus $R_{z\max} - R_{x\max}$) have opposite signs, which is consistent with expression (6) and the calculation shown in Fig. 2.

Now, when trying to quantify the ATMR amplitude from CIPTMR experiments, one has to take into account that the voltage drop across the barrier is not uniform between the electrical contacts. In the present semiquantitative approach, the spatial variation of this voltage drop can be estimated using the toy model of CIPTMR measurement proposed by Worledge and Trouilloud (Fig. 1 of Ref. [26]) (Fig. 5). The current is injected at the top surface of the top electrode and assumed to flow in parallel in the top and bottom electrodes which have respective resistance per square (R_T and R_B) and thickness (t_T and t_B). The current is leaking downwards from the top to bottom electrodes through the first half of the junction area and leaking upwards through the tunnel barrier over the second half of the junction area. Calling x the distance between the electrical contacts, L the width of the sample, RA the resistance \times area product of the tunnel barrier, and using the same resistance network as in Fig. 1 of Ref. [26], one can easily calculate the equivalent resistance measured in the CIPTMR

experiment:

$$R_{\text{eq}} = \left(\frac{x}{L}\right) \frac{R_T R_B}{R_T + R_B} \frac{1 + \frac{4RA}{x^2 R_B}}{1 + \frac{4RA}{x^2 (R_T + R_B)}}. \quad (9)$$

The voltage drop across the barrier then varies linearly as a function of the in-plane position ξ as

$$V_T(\xi) - V_B(\xi) = \left(\frac{V}{2 + \frac{x^2 R_B}{2RA}} \right) \frac{\xi}{2L}. \quad (10)$$

As a result, the Rashba coefficient α also varies in a similar linear fashion. The TAMR and ATMR being proportional to α^2 , the spatial averaging of the parabolic variation of the ATMR effect should lead to an effectively measured ATMR amplitude twice lower than the one that would be obtained with uniform voltage drop across the barrier. Consequently, the weak difference in magnetoresistance amplitude measured in plane and out of plane (92.4 vs 88.3%) represents an ATMR of two times $4.6 \pm 32\%$ at room temperature, i.e., $9.2 \pm 64\%$. This is the right expected order of magnitude but the uncertainty is too large to reasonably try to extract a corresponding value of the spin-orbit constant.

The measured ATMR encompasses all possible spin-orbit contributions influencing the dependence of the spin-dependent transport across the tunnel barrier on magnetization orientation. From a theoretical point of view, we examined here in detail the possible role of Rashba effect across the tunnel barrier. However, another contribution may originate from magneto-Coulomb effect [28]. Due to spin-orbit interaction, the density of states along the MgO/CoFeB interface depends on the direction of magnetization with respect to the crystallographic axis. This yields electron redistributions which depend on whether the magnetization is oriented in plane or out of plane. This contributes to the TAMR effect and may also contribute to the ATMR effect. The measured ATMR amplitude must therefore be viewed as an upper limit of the investigated Rashba contribution.

In conclusion, the anisotropy of the TMR (ATMR) was investigated both theoretically and experimentally in MgO-based magnetic tunnel junctions. Theoretically, it was shown that under the model assumption, the ATMR amplitude has twice the TAMR amplitude measured in parallel configuration. This derives from the fact that the TAMR (expressed as absolute variation of current or conductance at given voltage) in P configuration is just opposite to the TAMR in AP configuration. These effects were semiquantitatively confirmed by experiments performed on MTJs having orthogonal anisotropies (one electrode having easy-plane anisotropy and the other having perpendicular-to-plane anisotropy). These spin-orbit effects are too weak to explain the large difference in TMR amplitude generally observed between in-plane magnetized MTJs (up to 600%) and out-of-plane magnetized MTJs (up to 350%). This difference is more likely related to differences in stack growth quality and thickness of the magnetic layers.

It would be interesting to repeat this type of measurements at higher bias voltage to single out the Rashba contribution

in the observed ATMR effect since this contribution should increase quadratically with the bias voltage. One could also try to enhance the ATMR effect by using barrier materials with larger spin-orbit constant taking advantage of the knowhow developed in the field of spin orbitronics, for instance, by

introducing large spin-orbit impurities (e.g., Bi) in the barrier [29,30].

This work was partly funded by European Research Council MAGICAL Advanced Grant No. 669204.

-
- [1] P. Wölfe and K. A. Muttalib, *Philos. Trans. R. Soc. A* **15**, 508 (2006).
 - [2] N. Nagaosa, *J. Phys. Soc. Jpn.* **75**, 042001 (2006).
 - [3] T. R. McGuire and R. I. Potter, *IEEE Trans. Magn.* **11**, 1018 (1975).
 - [4] P. Gambardella and I. M. Miron, *Philos. Trans. R. Soc. A* **369**, 3175 (2011).
 - [5] L. Liu, C.-F. Pai, Y. Li, H. W. Tseng, D. C. Ralph, and R. A. Buhrman, *Science* **336**, 555 (2012).
 - [6] A. N. Chantis, K. D. Belashchenko, E. Y. Tsymbal, and M. van Schilfgaarde, *Phys. Rev. Lett.* **98**, 046601 (2007).
 - [7] A. B. Shick, F. Máca, J. Mašek, and T. Jungwirth, *Phys. Rev. B* **73**, 024418 (2006).
 - [8] J. D. Burton and E. Y. Tsymbal, *Phys. Rev. B* **93**, 024419 (2016).
 - [9] L. Gao, X. Jiang, S.-H. Yang, J. D. Burton, E. Y. Tsymbal, and S. S. P. Parkin, *Phys. Rev. Lett.* **99**, 226602 (2007).
 - [10] A. Matos-Abiague, M. Gmitra, and J. Fabian, *Phys. Rev. B* **80**, 045312 (2009).
 - [11] K. Wang, T. L. A. Tran, P. Brinks, J. G. M. Sanderink, T. Bolhuis, W. G. van der Wiel, and M. P. de Jong, *Phys. Rev. B* **88**, 054407 (2013).
 - [12] K. Wang, J. G. M. Sanderink, T. Bolhuis, W. G. van der Wiel, and M. P. de Jong, *Phys. Rev. B* **89**, 174419 (2014).
 - [13] Y. Y. Wang, C. Song, B. Cui, G. Y. Wang, F. Zeng, and F. Pan, *Phys. Rev. Lett.* **109**, 137201 (2012).
 - [14] W. H. Butler, X.-G. Zhang, T. C. Schulthess, and J. M. MacLaren, *Phys. Rev. B* **63**, 054416 (2001).
 - [15] M. N. Khan, J. Henk, and P. Bruno, *J. Phys.: Condens. Matter* **20**, 155208 (2008).
 - [16] B. Dieny, C. Cowache, A. Nossor, P. Dauguet, J. Chaussy, and P. Gandit, *J. Appl. Phys.* **79**, 6370 (1996).
 - [17] S. Ikeda, J. Hayakawa, Y. Ashizawa, Y. M. Lee, K. Miura, H. Hasegawa, M. Tsunoda, F. Matsukura, and H. Ohno, *Appl. Phys. Lett.* **93**, 082508 (2008).
 - [18] S. V. Karthik, Y. K. Takahashi, T. Ohkubo, K. Hono, H. D. Gan, S. Ikeda, and H. Ohno, *J. Appl. Phys.* **111**, 083922 (2012).
 - [19] M. Krounbi, V. Nikitin, D. Apalkov, J. Lee, X. Tang, R. Beach, D. Erickson, and E. Chen, *ECS Trans.* **69**, 119 (2015).
 - [20] Y. M. Lee, J. Hayakawa, S. Ikeda, F. Matsukura, and H. Ohno, *Appl. Phys. Lett.* **89**, 042506 (2006).
 - [21] S. Yuasa and D. D. Djayaprawira, *J. Phys. D* **40**, R337 (2007).
 - [22] J. C. Slonczewski, *Phys. Rev. B* **39**, 6995 (1989).
 - [23] A. Vedyayev, N. Ryzhanova, N. Strelkov, and B. Dieny, *Phys. Rev. Lett.* **110**, 247204 (2013).
 - [24] A. V. Vedyayev, M. S. Titova, N. V. Ryzhanova, M. Y. Zhuravlev, and E. Y. Tsymbal, *Appl. Phys. Lett.* **103**, 032406 (2013).
 - [25] N. Tezuka, N. Ikeda, F. Mitsunashi, and S. Sugimoto, *Appl. Phys. Lett.* **94**, 162504 (2009).
 - [26] D. C. Worledge and P. L. Trouilloud, *Appl. Phys. Lett.* **83**, 84 (2003).
 - [27] L. Cuchet, B. Rodmacq, S. Auffret, R. C. Sousa, and B. Dieny, *Appl. Phys. Lett.* **105**, 052408 (2014).
 - [28] A. Bernand-Mantel, P. Seneor, K. Bouzehouane, S. Fusil, C. Deranlot, F. Petroff, and A. Fert, *Nat. Phys.* **5**, 920 (2009).
 - [29] O. Mosendz, J. E. Pearson, F. Y. Fradin, G. E. W. Bauer, S. D. Bader, and A. Hoffmann, *Phys. Rev. Lett.* **104**, 046601 (2010).
 - [30] Y. Niimi, Y. Kawanishi, D. H. Wei, C. Deranlot, H. X. Yang, M. Chshiev, T. Valet, A. Fert, and Y. Otani, *Phys. Rev. Lett.* **109**, 156602 (2012).